Am J Transl Res 2022;14(8):5280-5294
www.ajtr.org /ISSN:1943-8141/AJTR0132252

Original Article

Curcumin prevents Alzheimer's disease progression by upregulating JMJD3

Yutong Wang[1*], Hong Zhang[2*], Linlin Hua[3], Zhen Wang[2], Shuang Geng[2], Hui Zhang[2], Zhilei Zeng[3], Jing Zhao[2], Xiaoyan Wang[2], Yunliang Wang[1,3]

[1]Qilu Medical College, Zibo, Shandong 255300, PR China; [2]Department of Neurology, 960th Hospital of PLA, Zibo 255300, Shandong, PR China; [3]Department of Neurology, The Second Affiliated Hospital of Zhengzhou University, Zhengzhou 450014, Henan, PR China. [*]Equal contributors.

Received February 22, 2021; Accepted March 9, 2022; Epub August 15, 2022; Published August 30, 2022

Abstract: The main purpose of this research was to explore the molecular mechanisms of Jumonji Domain-Containing Protein 3 (JMJD3) in Alzheimer's disease (AD) and to analyze its role in the anti-AD mechanism of curcumin (CUR). In the *in vitro* study of AD, JMJD3 overexpression promoted the trimethylation of histone H3 lysine 27 (H3K27me3), downregulated brain-derived neurotrophic factor (BDNF), improved the abnormality of mitochondrial stress response (MSR) markers, Aβ accumulation, increased cell proliferation and inhibited apoptosis. Upregulating BDNF also achieved above similar results. Knockout of JMJD3 could downregulate BDNF, upregulate the level of H3K27me3 methylation and inhibit MSR markers, while transfection of JMJD3 RNAi could counteract the upregulated effect of BDNF. Then, MSR activator could also improve AD. In addition, JMJD3 in AD *in vitro* models was obviously upregulated under CUR stimulation, and it triggered a series of reactions as mentioned above. In the *in vivo* study, the levels of JMJD3, the mRNA and protein levels of BDNF in the right brain tissues of AD mice were downregulated, the methylation of H3K27me3 increased, and the MSR markers (ClpP, HSP6, HSP-60, ATFS-1, etc.) were downregulated; the above indexes were improved in varying degrees with the intervention of CUR. Thus, we conclude that CUR can induce the upregulation of JMJD3 and improve BDNF expression by promoting the demethylation of H3K27me3, thereby maintaining the balance of MSR and thus, preventing AD development.

Keywords: JMJD3, H3K27me3, BDNF, curcumin, Alzheimer's disease

Introduction

Alzheimer's disease (AD) is a progressive neurodegenerative disease characterized by memory and cognitive loss, which has affected nearly 50 million people worldwide [1]. Its main pathological features are related to the deposition of brain amyloid-β (Aβ), and its prevalence is on the rise, which brings challenges to the medical care of the elderly [2, 3]. Up to now, there is no reliable and effective prevention or treatment, which brings a heavy public health burden to the society [4]. Hence, exploring the pathogenesis of AD and finding new drug targets are quite significant for its prevention and treatment.

The pathological mechanism of AD involves toxic effects caused by Aβ aggregation, such as mitochondrial dysfunction. Thus, minimizing mitochondrial dysfunction relating to Aβ aggregation has become a hot issue and breakthrough in AD treatment [5, 6]. It's known that mitochondrial dysfunction is accompanied by mitochondrial protein imbalance. A series of stress reactions reflecting this imbalance, also called mitochondrial stress response (MSR), such as mitochondrial unfolded protein response (UPRmt), mitochondrial autophagy and mitochondrial oxidative phosphorylation (OXPHOS), are key mechanisms to regulate mitochondrial protein balance [7, 8].

Brain-derived neurotrophic factor (BDNF), a member of the neurotrophic factor family, regulates brain physiological processes such as brain development, neuron regeneration and synaptic plasticity [9]. Its enhanced expression in AD is likely to improve MSR by activating UPR^{mt}, thus maintaining mitochondrial protein

balance, but the expression level is low in AD patients [10-12]. It is well acknowledged that a large number of genes are methylated in the pathological process of AD, which has epigenetic modification effects on the pathological process, which is mainly manifested by hypermethylation of gene promoter region and trimethylation of histone H3 lysine 27 (H3K27me3) [13, 14]. It has been reported that the methylation of H3K27Me3 in BDNF promoter region is negatively correlated with Jumonji Domain-Containing Protein 3 (JMJD3). When the level of JMJD3 decreases, the methylation of H3K27Me3 can increase, suggesting that JMJD3 can mediate the demethylation process of H3K27Me3 and promote BDNF expression [15, 16]. JMJD3, a selective demethylase containing Jumonji domain, has been reported to be involved in the regulation process of UPRmt; Deficiency of JMJD3 will lead to decreased level of UPR^{mt} and even reduced life span of nematode [17, 18].

Based on the above research results, we assume that the decrease of JMJD3 expression in AD may lead to the increase of methylation of H3K27Me3 in BDNF promoter region and the inhibition of BDNF expression. This will cause MSR abnormality and further aggravate the development and progression of AD.

Curcumin (CUR), the main component of traditional Chinese medicine turmeric, is a potential drug for AD treatment. It helps to inhibit the deposition and improve the depolymerization of Aβ, and is usually safe with multi-target effects [19-21]. However, it is unclear whether it has a regulatory effect on the JMJD3-BDNF axis. This research aimed to reveal the role of JMJD3 in the pathogenesis of AD and further explore the molecular mechanisms of CUR.

Materials and methods

Animals

Male APP/PS-1 transgenic AD mice (APP/PS-1 group, n = 40) and control wild-type C57BL/6 mice (WT group, n = 10) aged 6 months were purchased from the Institute of Medical Laboratory Animals, Chinese Academy of Medical Sciences. They were fed routinely in SPF-grade animal houses. This research was approved by the Animal Care and Protection Committee of Qilu Medical College (SA-184760), and the experimental steps were strictly in line with the animal care guidelines.

Animal grouping and drug intervention

All animals were divided into WT group (n = 10), APP/PS-1 group (n = 10) and CUR group (n = 10). For the CUR group, APP/PS-1 mice were peritoneally injected with CUR (Baoman Biotechnology Co., Ltd., Shanghai, China, C0190) at a dose of 200 mg/kg/d through a stereotactic instrument (Yuyan Scientific Co., Ltd., Shanghai, China) [22]. The treatment lasted for two weeks before the follow-up experiment.

Behavioral assessment

The cognitive function of mice was tested by the Morris water maze (MWM) 5 days after administration. First, the mice were randomized in four quadrants, their heads facing the wall were put in the water, and the time mice took to find a platform was measured. If they failed to reach the platform with 2 min, we then guided them to do so, and the mice were kept on the platform for 30 s, and the time in water was 120 s. After that, the mice were dried, placed in cages and trained twice a day. We recorded the time when mice searched for platforms in each quadrant and took the average escape latency in four quadrants as the final latency of the day. On the sixth day, the space probe test was carried out in the maze without platform, and the mice were placed at the marked position in the quadrant. The number of times when the mice passed the platform was recorded. It was tested twice, and the average value was the final result. The swimming speed was recorded. Afterwards, they were euthanized, and the right brain tissue samples were collected.

Pathological evaluation

We evaluated the pathological morphology and neuronal apoptosis level of brain tissues of mice mainly through hematoxylin and eosin (HE) staining and transferase-mediated deoxyuridine triphosphate-biotin nick end labeling (TUNEL) method. HE staining (Biolab Technology Co., Ltd., Beijing, China, ZN1970-KPC) and TUNEL detection kits (Qiming Biotechnology Co., Ltd., Shanghai, China, OX02752) were

used. The accumulation and clearance of Aβ were determined by immunohistochemistry.

In HE staining, paraffin-embedded mouse brain tissues were sliced into 4 μm sections. After being dewaxed in xylene, the tissues were then hydrated with ethanol in gradient concentration and washed with tap water. Finally, the slices were dyed with hematoxylin for 1 min. After being washed with tap water and intervened with 1% hydrochloric acid-ethanol (to distinguish them), the slices were put in 1% ammonia water and stained with eosin for 2 min after they turned blue for 30 s. Afterwards, the tissues were dehydrated by alcohol with gradient concentration, fixed in xylene and sealed with neutral balsam. Its morphological changes were observed under microscope.

In TUNEL assay, the antigens from brain slices after fixation were recovered, and the slices were paraffin embedded, dewaxed, hydrated with ethanol gradient concentration and washed at 80°C. Thereafter, the slices were incubated with proteinase K and TDT buffer successively. After being washed with PBS, they were cultivated with anti-digoxin and antiserum alkaline phosphatase complex at 37°C all night long. While after being washed in Tris-buffer, they were reversely dyed with corresponding reagents and finished with Tris-buffer. The apoptosis of rat hippocampus was observed under microscope, and the results were quantified by Image-Pro Plus. The apoptosis rate = TUNEL positive cells/total number of cells × 100%.

For IHC (immunohistochemistry) assay, the brain slices were dewaxed with xylene and graded ethanol solution, and then treated with 3% H_2O_2 for 10 min. Next, the anti-$A\beta_{1\text{-}40}$ antibody (Yubo Biotechnology Co., Ltd., Shanghai, China, YB-01103) was added for co-incubation overnight (dilution ratio 1:200) at 4°C. After being washed, it was incubated 20 min with biotinylated goat anti-mouse secondary antibody (Yanhui Biotechnology Co., Ltd., Shanghai, China, 115-035-003) at room temperature, and then intervened with avidin-biotin peroxidase complex reagent for 20 min. The peroxidase activity was observed with 3, 3'-diaminobenzidine (DAB), and then stained with hematoxylin. Finally, it was observed by optical microscope and quantitatively analyzed by evaluating the area of $A\beta_{1\text{-}40}$ plaque.

Cell culture and passage

The neuroblastoma SH-SY5Y cells (iPhase Pharmaceutical Services, Beijing, China) with APP Swedish K670N/M671L double mutation (APPswe) were used as *in vitro* AD cell model (AD group), and common SH-SY5Y without mutation were regarded as control group (CG). The cells were placed in DMEM/F-12 medium (Gaochuang Chemical Technology Co., Ltd., Shanghai, China) containing 10% FBS (Lianshuo Biotechnology Co., Ltd., Shanghai, China, A3160802 10 × 50 ml/box) and penicillin-streptomycin (Zhongqiao Xinzhou Biotechnology Co., Ltd., Shanghai, China, 0513-2). Before the experiment, the cells were passaged for three generations under the selective antibiotic of geneticin (Yaji Biotechnology Co., Ltd., Shanghai, China, YS-10555R) at 4 μg/ml.

Construction of over-expression and knockout models of JMJD3 and BNDF

The AD cell models (Hanheng Bioengineering Co., Ltd., Shanghai, China) with JMJD3 overexpression (JMJD3), JMJD3 knockdown (JMJD3 RNAi) and BNDF overexpression (BNDF) were constructed in AD cells by using adeno-associated virus (AAV) system and RNA interference technology (RNAi), and their empty vectors were used as negative controls (NC). Forty-eight hours after transfection, the successful construction was verified by qPCR and western blot (WB).

Drug intervention of in vitro AD cell models

According to different medication, AD cells was divided into two different subgroups, namely MSR activator nicotinamide ribose (NR) (Acmec Technology Co., Ltd., Shanghai, China.) and CUR, which were treated with 10 μM NR [23] and 20 μM [24] CUR respectively for two weeks.

qPCR

The total RNA of brain tissues was extracted by using high purity total RNA extraction kit (Angfei Biotechnology Co., Ltd., Guangzhou, China, RZ102), and cDNA was synthesized by Super M-MLV reverse transcriptase (BioTeke Corporation, Beijing, China, PR6502). Then, we amplified the reverse transcription products through SYBR Green reaction mixture (ThinkFar Technology Co., Ltd., Beijing, China, 4913-

Table 1. Primer sequence

Genes	Upstream primer	Downstream primer
JMJD3	5'-TCAGGAGAGGAAGGCCTCAG-3'	5'-AGCTGGGTATGGATGAGGGT-3'
BDNF	5'-CCAGGAGCGUGACAACAAUTT-3'	5'-AUUGUUGUCACGCUCCUGGTT-3'
ClpP	5'-GCCAAGCACACCAAACAGA-3'	5'-GGACCAGAACCTTGTCTAAG-3'
HSP6	5'-CACTCTGTCCCTCACTCGCCG-3'	5'-AACGGCCACAGCATCGGCTAAA-3'
HSP-60	5'-ATCCGAAGGGGTGTCATGATGG-3'	5'-GCAGAGATGGTTGCTACTTGTG-3'
ATFS-1	5'GACGGTCAATTGTGAATTGTC3'	5'-GCCTAGAAGCTTCCATCATGC-3'
PINK1	5'-GGAGGAGTATCTGATAGGGCAG-3'	5'-AACCCGGTGCTCTTTGTCAC-3'
PARK2	5'-AAAGGCCCCTGTCAAAGAGT-3'	5'-TTGTTGCGATCAGGTGCAAA-3'
BNIP3	5'-TCCAGCCTCGGTTTCTATTT-3'	5'-AGCTCTTGGAGCTACTCCGT-3'
P62	5'-GATGAGGAAGATCGCCTTGG-3'	5'-TCTGGCATCTGTAGGGACTG-3'
LC3(I)	5'-TACGAGCAGGAGAAAGACGAGG-3'	5'-GGCAGAGTARGGTGGGTTGGTG-3'
Cox5a	5'-TTAGTTTGTAGAGGGTTGGGATTATAGTA-3'	5'-ACCACAACACACTAA CTAAAACTAAAAA-3'
Cox2	5'-AGTCCCTGAGCATCTACGGT-3'	5'-AAAGGTGTCAGGCAGAAGGG-3'
Nd1	5'-GCCCATGTCTCCTATGCAGT-3'	5'-GCCCATGAGTACAGCCATTT-3'
Sdhc	5'-GAAAATAATTAGTAAATTAGTTAGGTAG-3'	5'-ACTAAAATCACCTCAACAACAAC-3'
GAPDH	5'-ACCACAGTCCATGCCATCAC-3'	5'-TTTAATG TCACGCACGATTTC-3'

914001). Soon afterwards, PCR reaction was conducted with quantitative PCR instrument (Image Trading Co., Ltd., Beijing, China, 100-131), and the data were determined by $2^{-\Delta\Delta CT}$ method (**Table 1**).

Western blot (WB)

The treated hippocampal tissues and cells were homogenized in RIPA lysis buffer (Runwell Industrial Co., Ltd., Shanghai, China, N653-100ML). After the sample was centrifugated at 1500xg, 4°C for 10 min, the supernatant was collected, and the protein concentration was measured by BCA kit (Biolab Technology Co., Ltd., Beijing, China, GL1484). The protein was treated by SDS-PAGE (Neobio Science and Trade Co., Ltd., Beijing, China, WB1102) to move onto the polyvinylidene fluoride (PVDF) membrane (Weijin Biotechnology Co., Ltd., Shanghai, China, IPVH00010). The blot was sealed with 5% skimmed milk powder in TBST (Xinfan Biotechnology Co., Ltd., Shanghai, China, XF-P438), and incubated with primary antibodies (the dilution concentration was 1: 1000) including JMJD3, BDNF and GAPDH (Wuhan Fine Biotech Co., Ltd., China, FNab04-440, FNab10014, FNab03343) at 4°C for 12 h. After being washed with TBST, it was cultivated with HRP coupled secondary antibody (Saihongrui Biotechnology Co., Ltd., Nanjing, China, 330) for 1 h at indoor temperature. Proteins were visualized and quantitatively analyzed through enhanced chemiluminescence (ECL) reagent (Huzhen Industrial Co., Ltd., Shanghai, China, HZ-F252), chemiluminescence imaging system (Xinyu Biotechnology Co., Ltd., Shanghai, China, XY-I600C) and Quantity One.

qPCR-chromatin immunoprecipitation (ChIP-qPCR)

Firstly, DNA-protein complex reacted with 1% formaldehyde for 15 min. The immune complexes were formed with nonspecific IgG against BDNF, H3K27me3 and JMJD3. Next, DNA in the complex was eluted and purified. Finally, the BDNF promoter was detected by PCR.

Cell proliferation assay

We measured cell proliferation by cell counting kit 8 (CCK-8) (Jingke Chemical Technology Co., Ltd., Shanghai, China, CK04-2). In the first place, the cells in logarithmic phase were inoculated into a 96-well plate (6×10^3 cells/well). In the second place, they were cultured i n 10% CCK-8 for 1 h, and the absorbance at 450 nm was measured by microplate reader (Yanhui Biotechnology Co., Ltd., Shanghai, China, HBS-1096A).

Determination of apoptosis

Annexin V-FITC/PI fluorescence double staining apoptosis detection kit (Sanshu Biotechnology Co., Ltd., Shanghai, China, BYT0035)

was applied. The washed and digested APPswe SH-SY5Y cells were centrifuged at 1500xg, 4°C for 10 min, and then suspended in 100 μL binding buffer (1 × 10^5 cells). Subsequently, they were incubated with 5 μL annexin V-FITC and 5 μL PI for 15 min. Finally, we quantitatively analyzed the apoptosis by FACSCalibur flow cytometry (Shiwei Experimental Instrument Technology Co., Ltd., Shanghai, China) within 1 h.

Statistical analysis

All data were statistically analyzed, and the pictures were generated by GraphPad Prism 6. All experiments were independently conducted at least 3 times, and the numerical value was expressed as mean ± standard deviation (S ± D). We compared the differences between multiple groups by one-way ANOVA followed with Dunnett's or Bonferroni post hoc analysis. $P < 0.05$ was considered to be statistically marked.

Results

Construction of in vitro AD model and abnormal expressions of JMJD3, H3K27me3 and BDNF

Compared with the CG, we found that Aβ in the cells of AD group accumulated dramatically (**Figure 1A**), cell proliferation decreased (**Figure 1B**), and neuron apoptosis level increased significantly (**Figure 1C**). On the other hand, the mRNA and protein levels of JMJD3 and BDNF in the AD group were remarkably lower than those in the CG (**Figure 1D-G**), while the level of BDNF promoter H3K27me3 was higher than that in the CG (**Figure 1H**). The above results indicate that the *in vitro* AD cell model had obvious AD characteristics, which were also accompanied by JMJD3, H3K27me3 and BDNF abnormalities (**Figure 1**).

Upregulating JMJD3 suppressed the progression of AD in cell model

To verify our conjecture, we constructed the overexpression models of JMJD3, and verified the transfection efficiency by qPCR and WB (**Figure 2A**, **2B**). Upregulating JMJD3 could upregulate BDNF (**Figure 2C**, **2D**), downregulate the methylation of H3K27me3 (**Figure 2E**), decrease the accumulation of Aβ (**Figure 2F**), increase cell proliferation level, inhibit apoptosis (**Figure 2G**, **2H**) and upregulate the expression levels of MSR markers (**Figure 2I**). The above results indicate that up-regulating JMJD3 suppressed AD progression in cell model by increasing BDNF expression and inhibiting H3K27me3 methylation (**Figure 2**).

Upregulating BDNF suppressed AD progression in AD cell model

We constructed the overexpression model of BDNF, carried JMJD3 RNAi on the basis of this model, and verified the transfection efficiency of BDNF by qPCR and WB (**Figure 3A**, **3B**). The results showed that upregulating BDNF showed similar anti-AD effects as upregulation of JMJD3. That was, compared with AD group, the accumulation of Aβ in the BDNF group decreased (**Figure 3C**), the level of cell proliferation increased (**Figure 3D**), the level of neuronal apoptosis decreased (**Figure 3E**), and the levels of MSR markers increased (**Figure 3F**).

BDNF was upregulated, and then a knock-down model of JMJD3 was constructed. The data revealed that compared with BDNF group, the changes of the above indexes in the BDNF + JMJD3 RNAi group were dramatically offset. There was no marked difference to the AD group, which indicated that JMJD3 silence could downregulate BDNF and offset the anti-AD effect after BDNF upregulation. The above results suggest that upregulating BDNF also has anti-AD effect, and the anti-AD mechanism of BDNF is positively regulated by JMJD3 (**Figure 3**).

MSR activator promoted AD progression of AD cells

We proved the role of MSR activator NR in anti-AD process. The data signified that compared with AD group, the NR treatment promoted the levels of MSR markers in different degrees (**Figure 4A**); further, there was a decreased level of Aβ (**Figure 4B**), and increased cell proliferation level increased (**Figure 4C**), while the neuron apoptosis level decreased (**Figure 4D**). The above results indicate that NR, as an activator of MSR, can restrain AD process by improving MSR balance (**Figure 4**).

CUR induced JMJD3 and suppressed AD progression in in vitro cell models

Previous research confirmed that upregulating JMJD3 could suppress the progression of AD

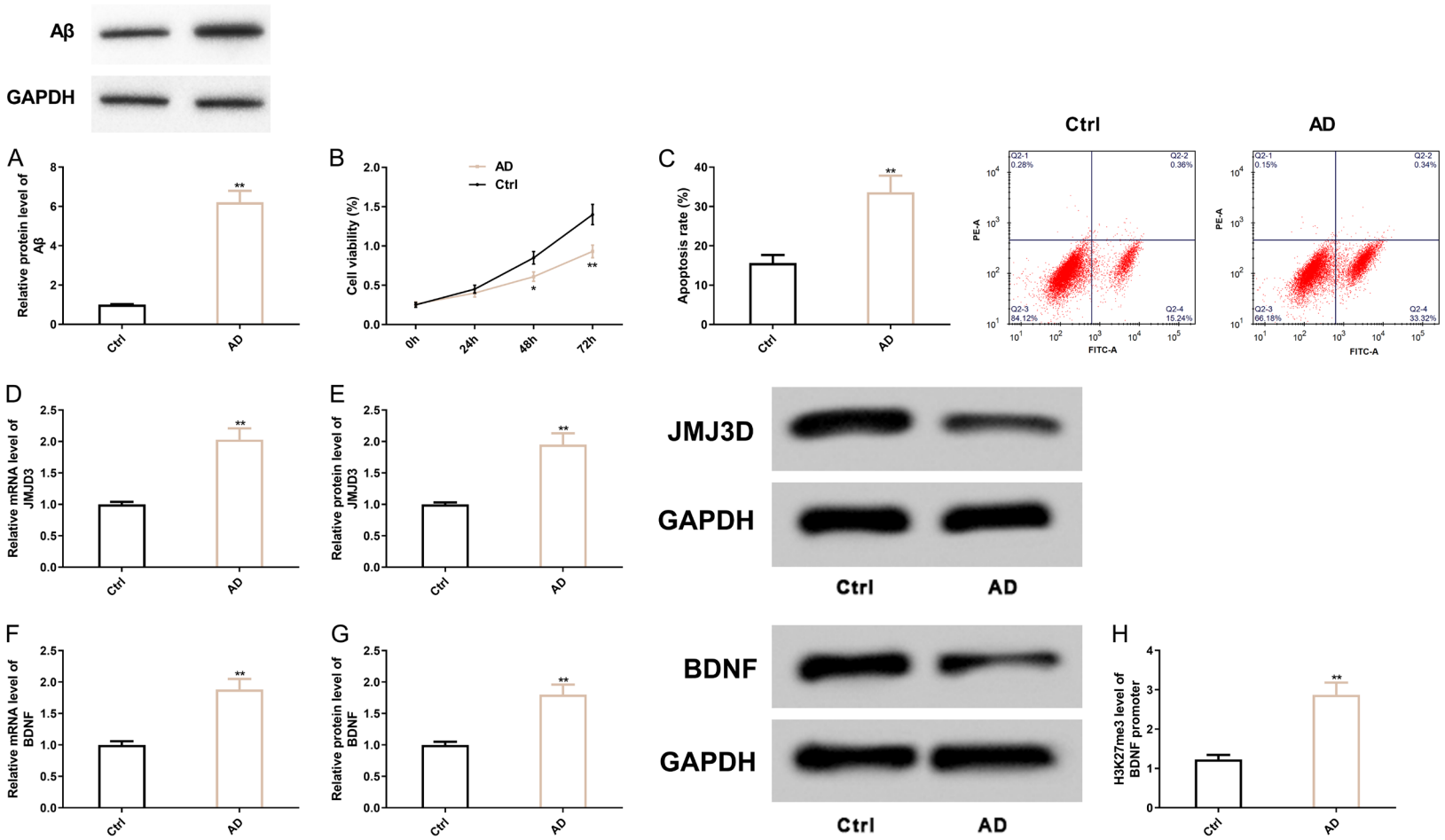

Figure 1. Construction of AD models *in vitro* and abnormal expressions of JMJD3, H3K27me3 and BDNF. Aβ accumulation was detected by WB (A); cell proliferation (B) was tested by CCK-8 method; apoptosis level was analyzed by Flow cytometry (C); the mRNA and protein levels of JMJD3 and BDNF (D-G) were tested by qPCR and WB; the level of H3K27me3 in BDNF promoter region was assessed by ChIP-qPCR (H). Note: compared with Ctrl, *means $P < 0.05$; **means $P < 0.01$; compared with AD.

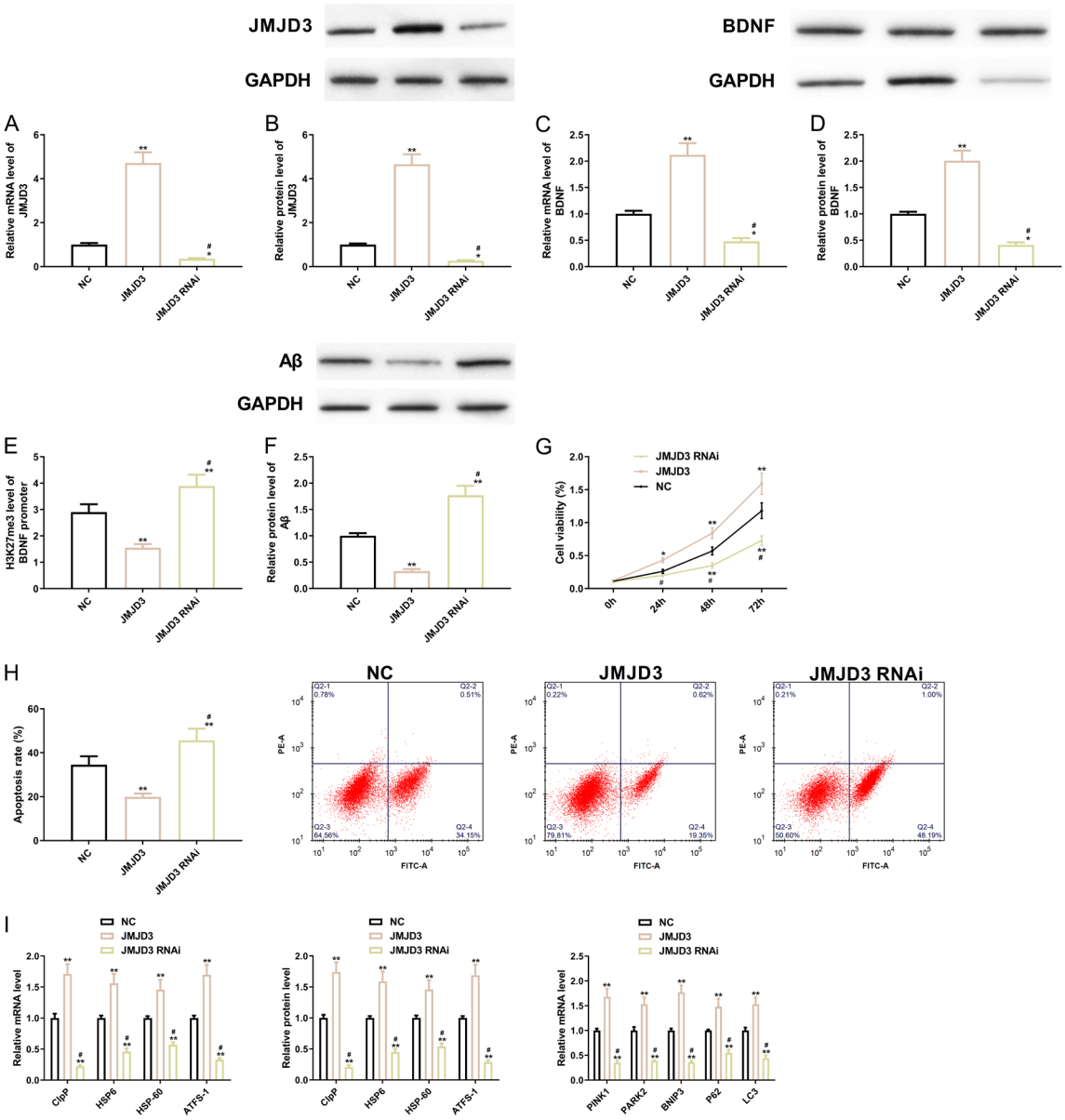

Figure 2. Upregulating JMJD3 suppressed AD progression *in vitro* models. mRNA and protein expressions of JMJD3 and BDNF (A-D) were examined by qPCR and WB; methylation of H3K27me3 was detected by ChIP-qPCR (E); Aβ accumulation (F) was tested by WB; cell proliferation and neuronal apoptosis were tested by CCK-8 method and Flow cytometry (G, H); MSR markers (I) were tested by qPCR. Note: compared with Ctrl, *means $P < 0.05$; **means $P < 0.01$; compared with AD, #means $P < 0.05$.

by upregulating BDNF and MSR markers. Furthermore, we verified whether CUR could induce JMJD3 and suppress AD progression. It showed that JMJD3 in *in vitro* AD cell model was dramatically upregulated under CUR stimulation (**Figure 5A**, **5B**), and triggered the series of cascade reactions mentioned above. Namely, the mRNA and protein expressions of BDNF was markedly upregulated (**Figure 5C**, **5D**), and the methylation of H3K27me3 (**Figure 5E**) and accumulation of Aβ were reduced (**Figure 5F**). The level of cell proliferation increased (**Figure 5G**) and neuronal apoptosis decreased (**Figure 5H**), and the MSR markers were upregulated in different degrees (**Figure 5I**). This suggests that CUR can suppress AD progression in *in vitro* cell model by inducing JMJD3 (**Figure 5**).

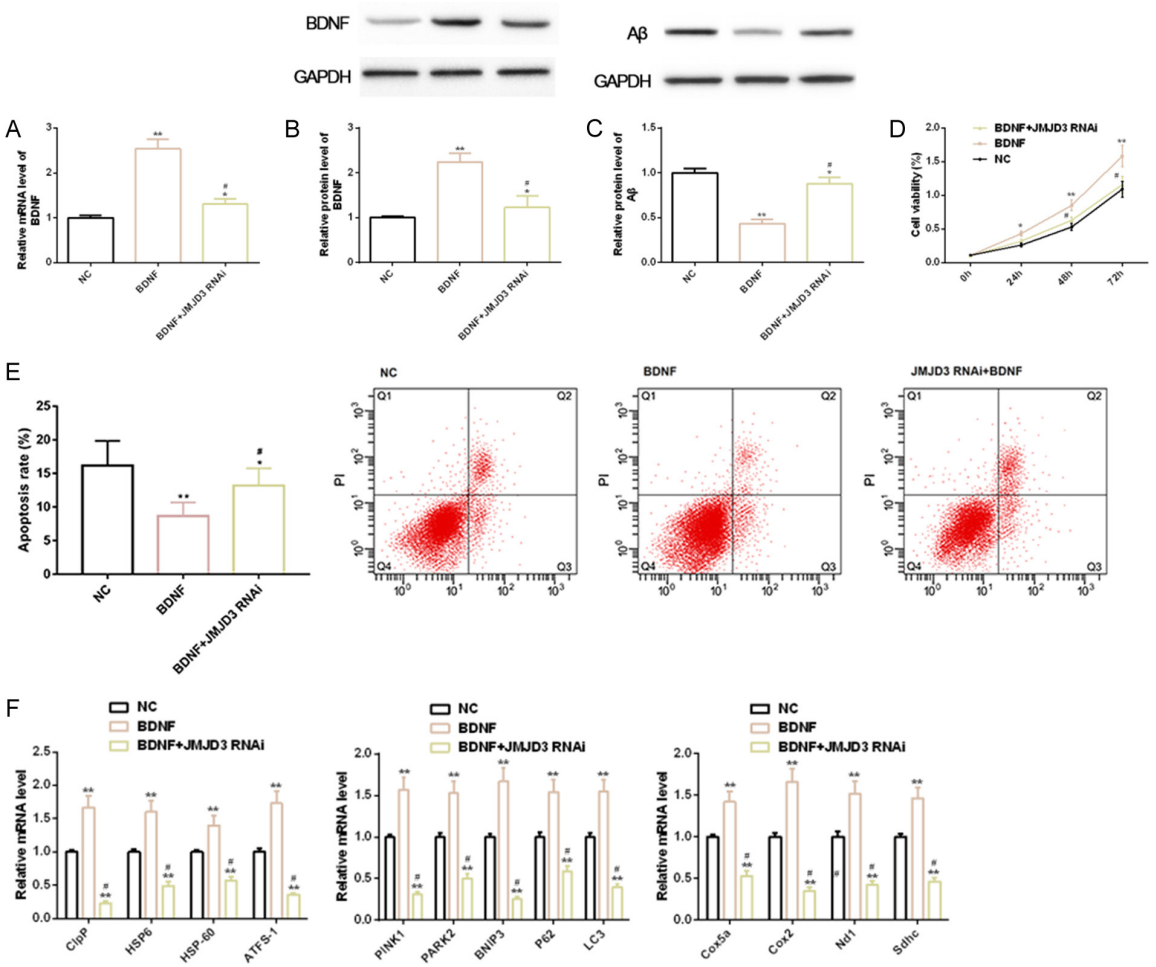

Figure 3. Upregulation of BDNF suppressed AD progression of *in vitro* cell models. The transfection efficiency of BDNF was detected by qPCR and WB (A, B); Aβ accumulation was tested by WB (C); cell proliferation and neuronal apoptosis were detected by CCK-8 method and Flow cytometry (D, E); MSR markers were detected by qPCR (F). Note: compared with Ctrl, *means $P < 0.05$; **means $P < 0.01$; compared with AD, #means $P < 0.05$.

Improvement of pathological conditions under CUR intervention

The cognitive impairments of AD mouse models were evaluated through pathological and behavioral analysis. Compared with WT group, the motor and cognitive functions of the mice in APP/PS-1 group were obviously inhibited in MWM test, while the above behavioral indexes were improved in different degrees under CUR intervention, which was mainly reflected in the shortening of escape latency, and the increase of platform crossing times, target quadrant staying time and swimming speed (**Figure 6A-D**). Pathological study revealed that compared with WT group, Aβ was dramatically accumulated in the APP/PS-1 group (**Figure 6E**). There were remarkable pathological changes in cortex, hippocampus and other brain tissues (**Figure 6F**, **6G**), and the level of neuronal apoptosis increased (**Figure 7**). However, under the treatment of CUR, the above pathological results were improved to various degrees. The above results indicate that the AD mouse models were successfully constructed and CUR attenuated the pathological deterioration in AD mice (**Figures 6**, **7**).

Effect of CUR on JMJD3, H3K27me3 and BDNF of AD mouse models

In addition, we detected the levels of JMJD3, H3K27me3 and BDNF in AD mouse models. The results manifested that the mRNA and protein levels of JMJD3 and BDNF in the APP/PS-1 group were lower than those in the WT group

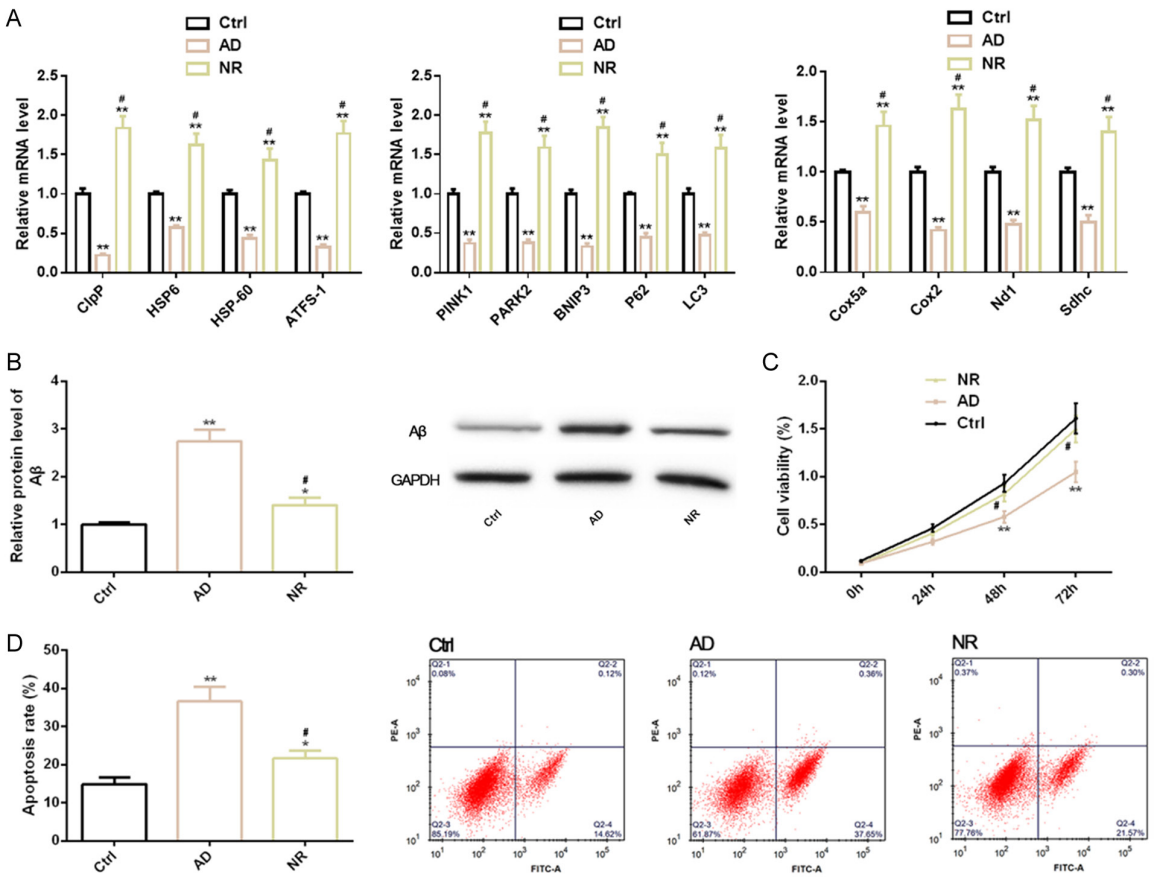

Figure 4. MSR activator suppressed AD progression in *in vitro* cell models. MSR markers (A) were detected by qPCR and WB; Aβ accumulation (B) was tested by WB; cell proliferation and neuronal apoptosis were tested by CCK-8 method and Flow cytometry (C, D). Note: compared with Ctrl, *means $P < 0.05$; **means $P < 0.01$; compared with AD, #means $P < 0.05$.

(**Figure 8A-D**), and the H3K27me3 level was obviously higher than that in the WT group (**Figure 8E**). However, all the above indexes were reversed to various degrees under the treatment of CUR. It suggests that the abnormal expression of JMJD3, H3K27me3 and BDNF in AD *mice* was regulated by CUR (**Figure 8**).

CUR increased MSR of AD mouse models

MSR is related to Aβ accumulation caused by mitochondrial dysfunction [25]. So, we explored the effect of CUR on MSR of APP/PS-1 mice. Compared with the WT group, the UPRmt in dexes such as ClpP, HSP6, HSP-60, ATFS-1 (**Figure 9A**) and mitochondrial autophagy markers PINK1, PARK2, BNIP3, P62, LC3 in the APP/PS-1 group decreased (**Figure 9B**). The OXPHOS indexes such as Cox5a, Cox2, Nd1, Sdhc were markedly downregulated (**Figure 9C**). However, the above results were improved to various degrees under the treatment of CUR. This suggests that the MSR disorder in AD mice were recovered to some extent under the influence of CUR (**Figure 9**).

Discussion

Alzheimer's disease (AD) severely affects patients' quality of life in varying degrees. It mainly manifested as memory loss, cognitive impairment, life restriction etc [26-28]. The main pathological feature is abnormal protein deposition or plaque of Aβ. Although there have been a lot of researches on the pathogenesis of AD, the cognition of specific pathological process is still very limited [29, 30].

In this research, both *in vivo and in vitro* models of AD were verified. Our *in vitro* study

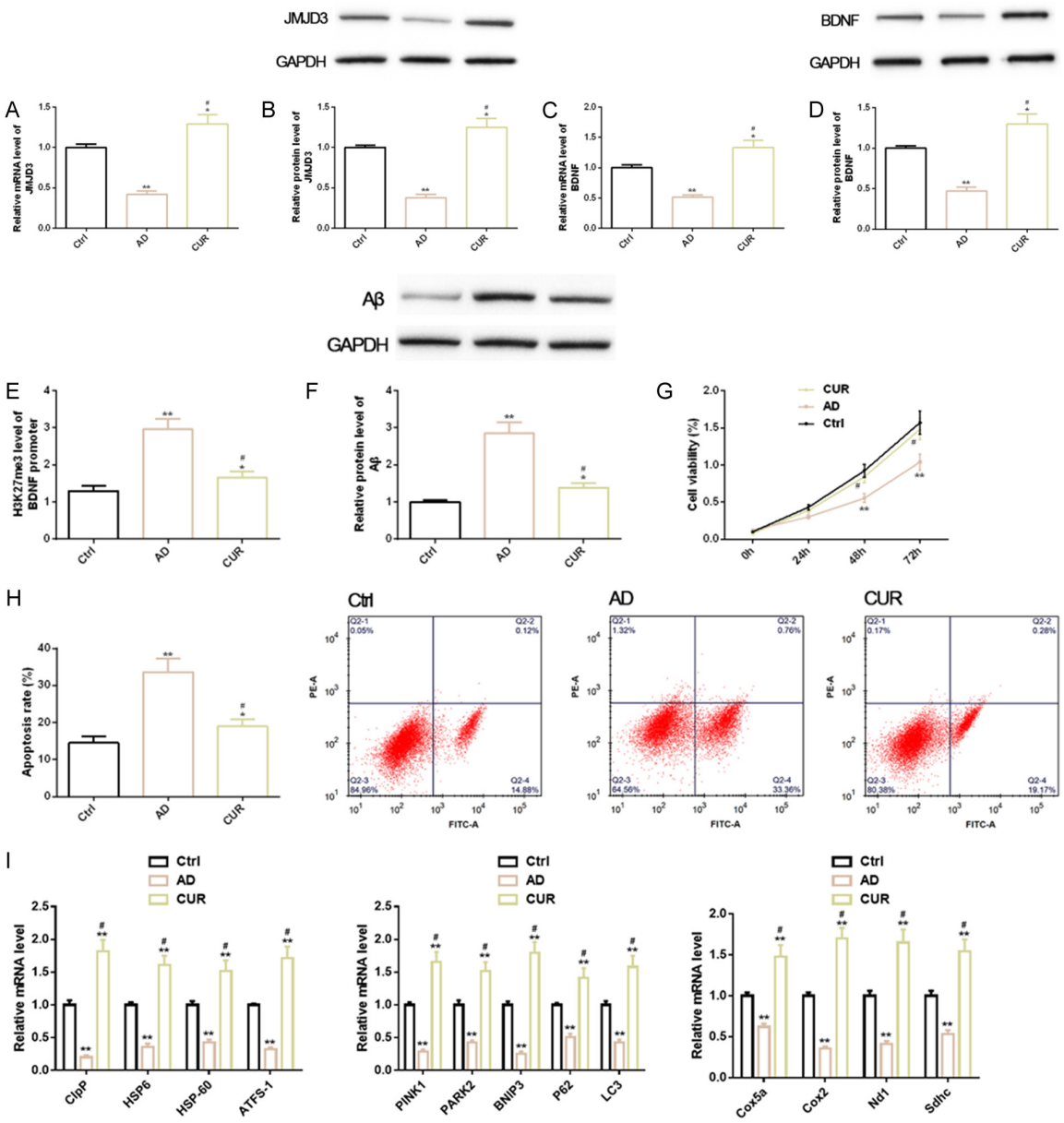

Figure 5. CUR can induce JMJD3 and improve the course of AD in vitro. mRNA and protein expressions of JMJD3 and BDNF were detected by qPCR and WB (A-D); H3K27me3 methylation was tested by ChIP-qPCR (E); Aβ accumulation (F) was detected by WB; cell proliferation and neuronal apoptosis (G, H) were tested by CCK-8 method and Flow cytometry; MSR markers were tested by qPCR (I). Note: compared with Ctrl, *means $P < 0.05$; **means $P < 0.01$; compared with AD, #means $P < 0.05$.

analyzed the anti-AD mechanism of JMJD3. APPswe SH-SY5Y cells were employed as an AD cell model, the successful construction of the model was verified by Aβ and molecular expression analyses, and there were abnormal H3K27me3 methylation levels in the promoters of JMJD3 and BDNF. Then, we found that upregulation of JMJD3 or BDNF, and administration of MSR activator NR or CUR could inhibit the pathological process of AD *in vitro*. Besides, we discovered that upregulating JMJD3 could promote BDNF expression, which was accompanied by decreased level of methylation of H3K27me3 in BDNF promoter region, which improves MSR and further restrains AD pathological changes. Most importantly, CUR had a positive regulatory effect on JMJD3, and it also activated a series of cascade reactions as mentioned before. Zhu X et al. [31] explained that CUR could exert analgesic effects by regu-

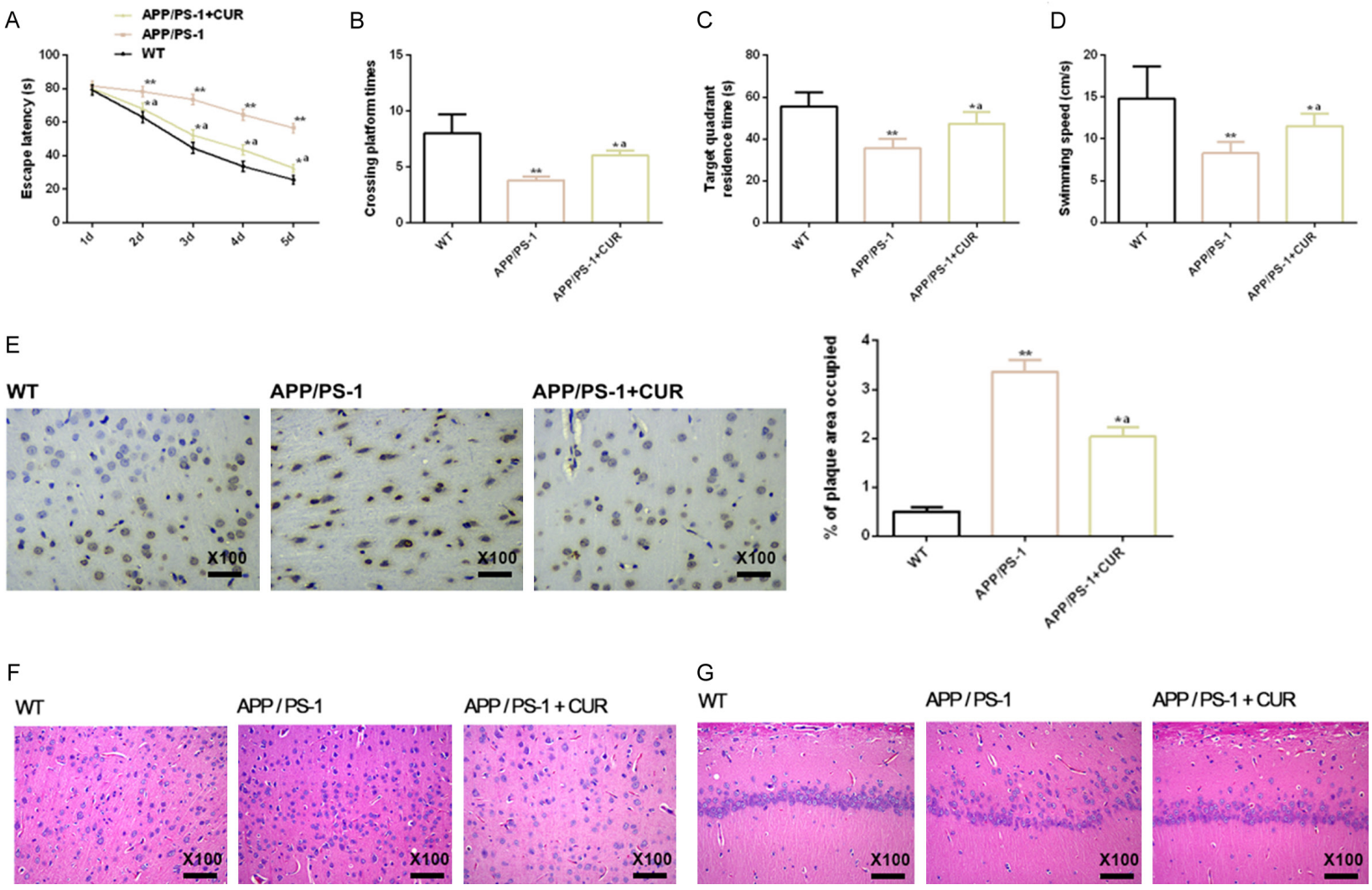

Figure 6. Establishment of AD mouse models and improvement of pathological conditions under CUR intervention. The cognitive function of AD mice was examined by MWM experiment (A-D); the accumulation of Aβ in AD mice was analyzed by immunohistochemistry (E); the pathological changes of brain tissues such as cortex and hippocampus was verified by HE staining (F, G). Note: compared with WT, *means $P < 0.05$; **means $P < 0.01$; compared with APP/PS-1.

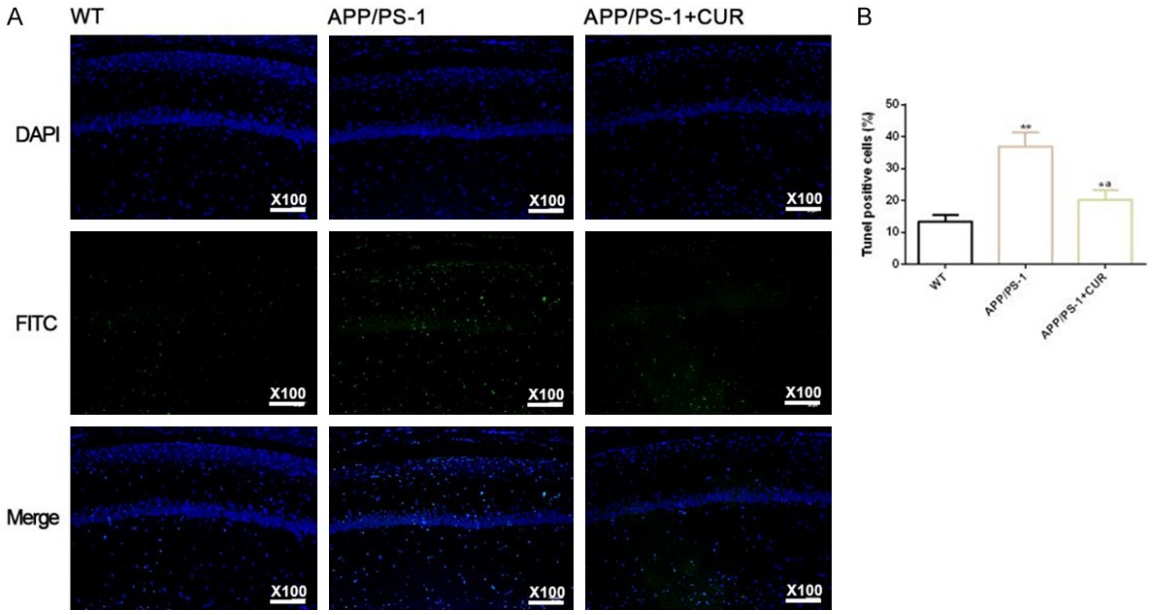

Figure 7. Neuronal apoptosis level in AD mouse model was detected by TUNEL staining. TUNEL experimental chart (A) and statistical analysis result (B). Note: compared with WT, *means $P < 0.05$; **means $P < 0.01$; compared with APP/PS-1, [a]means $P < 0.05$.

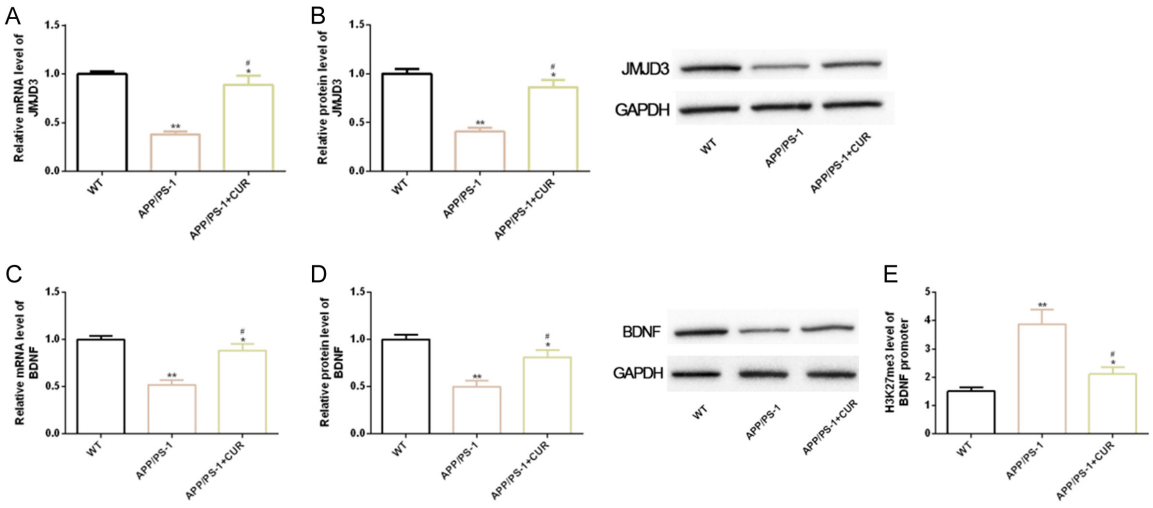

Figure 8. Effect of CUR on JMJD3, H3K27me3 and BDNF of AD mouse model. mRNA and protein expressions of JMJD3 and BDNF were detected by qPCR and WB (A-D); H3K27me3 level (E) in BDNF promoter region was examined by ChIP-qPCR. Note: compared with WT, *means $P < 0.05$; compared with APP/PS-1, #means $P < 0.01$.

lating the expression of BDNF in neuropathic pain rat models, which suggested that it had a certain regulatory effect on BDNF. Many studies have also clarified that CUR can regulate the methylation of H3K27me3 in the promoter region [32, 33].

We also analyzed the effect of CUR on the above cascade reaction *in vivo*. Firstly, the behavior and pathology were evaluated in AD mouse models, which confirmed the reliability of the model construction. In MWM test, the ability of spatial learning and memory of APP/PS-1 mice was obviously lower than that of WT mice. Compared with WT group, the cortex and hippocampus of the APP/PS-1 group showed typical pathological morphology of AD, and the level of neuronal apoptosis increased, and the level of protein Aβ highly relating to the pathogenesis of AD increased. On the other hand, AD

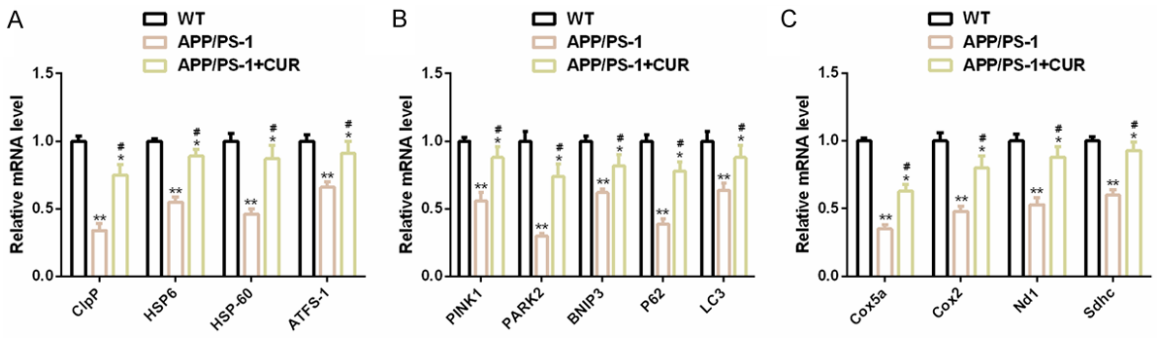

Figure 9. CUR increased the expressions of MSR markers of APP/PS-1 mice. The UPRmt indicators (A) such as ClpP, HSP6, HSP-60 and ATFS-1, the mitochondrial autophagy markers (B) PINK1, PARK2, BNIP3, P62 and LC3, and the OXPHOS indicators (C) Cox5a, Cox2, Nd1 and Sdhc were detected by qPCR. Note: compared with WT, *means $P < 0.05$; **means $P < 0.01$; compared with APP/PS-1, $^{\#}$means $P < 0.05$.

mouse models were intervened by CUR, and the above pathological changes were remarkably improved, suggesting that CUR had anti-AD effect, which has also been demonstrated in previous studies [34, 35]. What's more, compared with the WT group, the APP/PS-1 mice had lower levels of JMJD3, BDNF and higher methylation of H3K27me3. It could be improved by CUR, which indicated that CUR could regulate the levels of JMJD3, BDNF and H3K27me3 promoter region of BDNF. Popov N and Gil J [36] pointed out that JMJD3 could indirectly control INK4b-ARF-INK4a locus through the interaction site with Polycomb inhibitory complex, and then partially manipulate antisense non-coding RNA in the INK4 locus (ANRIL) to influence AD process. According to previous reports, BDNF is a crucial regulator of neuronal activity and memory process. The serum BDNF level of AD patients is dramatically lower than that of healthy subjects, suggesting that its abnormal level may facilitate AD process, which is similar to our research [37, 38]. Furthermore, JMJD3 is a key factor in the regulation of demethylation of H3K27me3 in BDNF promoter region. Improving JMJD3 expression helps to reduce the methylation level of H3K27me3 in BDNF promoter region, stimulate the transcription of BDNF, and then improve the neuropathy of central nervous system [39]. MSR research found that the indexes of UPR^{mt}, mitochondrial autophagy and OXPHOS in the APP/PS-1 group were markedly lower than those in the WT group but increased under the action of CUR, which indicated that CUR could improve MSR and maintain mitochondrial protein balance. Many studies have shown that activation of UPR^{mt} after mitochondrial protein imbalance can help alleviate MSR, which is mainly reflected in the upregulation of markers such as ClpP, HSP6, HSP-60 and ATFS-1, accompanied by the upregulation of mitochondrial autophagy markers PINK1, PARK2, BNIP3, P62, LC3 and OXPHOS markers Cox5a, Cox2, Nd1 and Sdhc. These results indicate that UPRmt, mitochondrial autophagy and OXPHOS play a synergistic role in maintaining mitochondrial protein balance and function [7, 40, 41].

The above research confirms that upregulating JMJD3 improves MSR by reducing the methylation level of H3K27me3 and promoting BDNF expression, thus inhibiting AD progression. The innovation of this research is that we analyzed and confirmed the anti-AD molecular mechanism of CUR by inducing JMJD3 and further promoting BDNF expression. Nevertheless, there is still room for improvement. It's a preliminary research, and the number of animal samples needs to be further increased. Secondly, the research on the MSR-related pathways can be further supplemented to further explore the potential molecular mechanism.

In brief, we first proposed that upregulating JMJD3 could improve the BDNF level by inducing demethylation of H3K27me3, thereby maintaining the MSR balance and preventing AD development and progression. JMJD3 could also be induced by CUR. So, it further uncovered the molecular mechanism of CUR in treating AD, providing a solid theoretical basis for its clinical application.

Acknowledgements

Natural Fund of Shandong Province (ZR2019-MH065).

Disclosure of conflict of interest

None.

Address correspondence to: Yunliang Wang, Qilu Medical College, No. 246, West Waihuan Road, Boshan Economic and Technological Development Zone, Zibo 255300, Shandong, PR China. Tel: 0533-2829222; E-mail: yunliangwang234@163.com

References

[1] Poirier Y, Grimm A, Schmitt K and Eckert A. Link between the unfolded protein response and dysregulation of mitochondrial bioenergetics in Alzheimer's disease. Cell Mol Life Sci 2019; 76: 1419-1431.

[2] Lozupone M, La Montagna M, D'Urso F, Piccininni C, Rinaldi A, Beghi M, Cornaggia CM, Sardone R, Solfrizzi V, Daniele A, Seripa D, Giannelli G, Bellomo A and Panza F. The challenge of antidepressant therapeutics in Alzheimer's disease. Adv Exp Med Biol 2020; 1260: 267-281.

[3] Ke S, Yang Z, Yang F, Wang X, Tan J and Liao B. Long noncoding RNA NEAT1 aggravates abeta-induced neuronal damage by targeting miR-107 in Alzheimer's disease. Yonsei Med J 2019; 60: 640-650.

[4] Feng L, Liao YT, He JC, Xie CL, Chen SY, Fan HH, Su ZP and Wang Z. Plasma long non-coding RNA BACE1 as a novel biomarker for diagnosis of Alzheimer disease. BMC Neurol 2018; 18: 4.

[5] Gu C, Chen C, Wu R, Dong T, Hu X, Yao Y and Zhang Y. Long noncoding RNA EBF3-AS promotes neuron apoptosis in Alzheimer's disease. DNA Cell Biol 2018; 37: 220-226.

[6] Dixit S, Fessel JP and Harrison FE. Mitochondrial dysfunction in the APP/PSEN1 mouse model of Alzheimer's disease and a novel protective role for ascorbate. Free Radic Biol Med 2017; 112: 515-523.

[7] Sorrentino V, Romani M, Mouchiroud L, Beck JS, Zhang H, D'Amico D, Moullan N, Potenza F, Schmid AW, Rietsch S, Counts SE and Auwerx J. Enhancing mitochondrial proteostasis reduces Amyloid-Beta proteotoxicity. Nature 2017; 552: 187-193.

[8] Ruan L, Zhou C, Jin E, Kucharavy A, Zhang Y, Wen Z, Florens L and Li R. Cytosolic proteostasis through importing of misfolded proteins into mitochondria. Nature 2017; 543: 443-446.

[9] Chen KW and Chen L. Epigenetic regulation of BDNF gene during development and diseases. Int J Mol Sci 2017; 18: 3.

[10] Martinez G, Vidal RL, Mardones P, Serrano FG, Ardiles AO, Wirth C, Valdes P, Thielen P, Schneider BL, Kerr B, Valdes JL, Palacios AG, Inestrosa NC, Glimcher LH and Hetz C. Regulation of memory formation by the transcription factor XBP1. Cell Rep 2016; 14: 1382-1394.

[11] Saito A, Cai L, Matsuhisa K, Ohtake Y, Kaneko M, Kanemoto S, Asada R and Imaizumi K. Neuronal activity-dependent local activation of dendritic unfolded protein response promotes expression of brain-derived neurotrophic factor in cell soma. J Neurochem 2018; 144: 35-49.

[12] Rao JS, Keleshian VL, Klein S and Rapoport SI. Epigenetic modifications in frontal cortex from Alzheimer's disease and bipolar disorder patients. Transl Psychiatry 2012; 2: e132.

[13] Delgado-Morales R and Esteller M. Opening up the DNA methylome of dementia. Mol Psychiatry 2017; 22: 485-496.

[14] Watson CT, Roussos P, Garg P, Ho DJ, Azam N, Katsel PL, Haroutunian V and Sharp AJ. Genome-wide DNA methylation profiling in the superior temporal gyrus reveals epigenetic signatures associated with Alzheimer's disease. Genome Med 2016; 8: 5.

[15] Fernandez-Monreal M, Brown TC, Royo M and Esteban JA. The balance between receptor recycling and trafficking toward lysosomes determines synaptic strength during long-term depression. J Neurosci 2012; 32: 13200-13205.

[16] Palomer E, Carretero J, Benvegnu S, Dotti CG and Martin MG. Neuronal activity controls Bdnf expression via polycomb de-repression and CREB/CBP/JMJD3 activation in mature neurons. Nat Commun 2016; 7: 11081.

[17] De Santa F, Totaro MG, Prosperini E, Notarbartolo S, Testa G and Natoli G. The histone H3 lysine-27 demethylase Jmjd3 links inflammation to inhibition of polycomb-mediated gene silencing. Cell 2007; 130: 1083-1094.

[18] Merkwirth C, Jovaisaite V, Durieux J, Matilainen O, Jordan SD, Quiros PM, Steffen KK, Williams EG, Mouchiroud L, Tronnes SU, Murillo V, Wolff SC, Shaw RJ, Auwerx J and Dillin A. Two conserved histone demethylases regulate mitochondrial stress-induced longevity. Cell 2016; 165: 1209-1223.

[19] Joe B, Vijaykumar M and Lokesh BR. Biological properties of curcumin-cellular and molecular mechanisms of action. Crit Rev Food Sci Nutr 2004; 44: 97-111.

[20] Begum AN, Jones MR, Lim GP, Morihara T, Kim P, Heath DD, Rock CL, Pruitt MA, Yang F, Hudspeth B, Hu S, Faull KF, Teter B, Cole GM and Frautschy SA. Curcumin structure-function, bioavailability, and efficacy in models of neuroinflammation and Alzheimer's disease. J Pharmacol Exp Ther 2008; 326: 196-208.

[21] Ma QL, Yang F, Rosario ER, Ubeda OJ, Beech W, Gant DJ, Chen PP, Hudspeth B, Chen C, Zhao Y, Vinters HV, Frautschy SA and Cole GM. Beta-amyloid oligomers induce phosphorylation of tau and inactivation of insulin receptor

substrate via c-Jun N-terminal kinase signaling: suppression by omega-3 fatty acids and curcumin. J Neurosci 2009; 29: 9078-9089.
[22] Feng HL, Dang HZ, Fan H, Chen XP, Rao YX, Ren Y, Yang JD, Shi J, Wang PW and Tian JZ. Curcumin ameliorates insulin signalling pathway in brain of Alzheimer's disease transgenic mice. Int J Immunopathol Pharmacol 2016; 29: 734-741.
[23] Gong B, Pan Y, Vempati P, Zhao W, Knable L, Ho L, Wang J, Sastre M, Ono K, Sauve AA and Pasinetti GM. Nicotinamide riboside restores cognition through an upregulation of proliferator-activated receptor-gamma coactivator 1alpha regulated beta-secretase 1 degradation and mitochondrial gene expression in Alzheimer's mouse models. Neurobiol Aging 2013; 34: 1581-1588.
[24] Qian W, Li H, Pan N and Zhang C. Curcumin treatment is associated with increased expression of the N-methyl-D-aspartate receptor (NMDAR) subunit, NR2A, in a rat PC12 cell line model of Alzheimer's disease treated with the acetyl Amyloid-Beta peptide, ABeta (25-35). Med Sci Monit 2018; 24: 2693-2699.
[25] Costa RO, Ferreiro E, Oliveira CR and Pereira CM. Inhibition of mitochondrial cytochrome c oxidase potentiates Abeta-induced ER stress and cell death in cortical neurons. Mol Cell Neurosci 2013; 52: 1-8.
[26] Bature F, Guinn BA, Pang D and Pappas Y. Signs and symptoms preceding the diagnosis of Alzheimer's disease: a systematic scoping review of literature from 1937 to 2016. BMJ Open 2017; 7: e015746.
[27] Bryukhovetskiy AS. Translational experience of 28 years of use of the technologies of regenerative medicine to treat complex consequences of the brain and spinal cord trauma: results, problems and conclusions. J Neurorestoratology 2018; 6: 99-114.
[28] Fan J, Milosevic R, Li JF, Bai JJ and Zhang YQ. The impact of neuroimaging advancement on neurocognitive evaluation in pediatric brain tumor survivors: a review. Brain Science Advances 2019; 5: 117-27.
[29] Jiang Y, Xu B, Chen J, Sui Y, Ren L, Li J, Zhang H, Guo L and Sun X. Micro-RNA-137 inhibits Tau hyperphosphorylation in Alzheimer's disease and targets the CACNA1C gene in transgenic mice and human neuroblastoma SH-SY5Y cells. Med Sci Monit 2018; 24: 5635-5644.
[30] Yang YH, Fuh JL and Mok VCT. Vascular contribution to cognition in stroke and Alzheimer r's disease. Brain Science Advances 2018; 4: 39-48.
[31] Zhu X, Li Q, Chang R, Yang D, Song Z, Guo Q and Huang C. Curcumin alleviates neuropathic pain by inhibiting p300/CBP histone acetyltransferase activity-regulated expression of BDNF and cox-2 in a rat model. PLoS One 2014; 9: e91303.
[32] Shu L, Khor TO, Lee JH, Boyanapalli SS, Huang Y, Wu TY, Saw CL, Cheung KL and Kong AN. Epigenetic CpG demethylation of the promoter and reactivation of the expression of Neurog1 by curcumin in prostate LNCaP cells. AAPS J 2011; 13: 606-614.
[33] Ma L, Zhang X, Wang Z, Huang L, Meng F, Hu L, Chen Y and Wei J. Anti-cancer effects of curcumin on myelodysplastic syndrome through the inhibition of enhancer of zeste homolog-2 (EZH2). Curr Cancer Drug Targets 2019; 19: 729-741.
[34] Teter B, Morihara T, Lim GP, Chu T, Jones MR, Zuo X, Paul RM, Frautschy SA and Cole GM. Curcumin restores innate immune Alzheimer's disease risk gene expression to ameliorate Alzheimer pathogenesis. Neurobiol Dis 2019; 127: 432-448.
[35] Li J, Han Y, Li M and Nie C. Curcumin promotes proliferation of adult neural stem cells and the birth of neurons in Alzheimer's disease mice via notch signaling pathway. Cell Reprogram 2019; 21: 152-161.
[36] Popov N and Gil J. Epigenetic regulation of the INK4b-ARF-INK4a locus: in sickness and in health. Epigenetics 2010; 5: 685-690.
[37] Angelucci F, Cechova K, Prusa R and Hort J. Amyloid beta soluble forms and plasminogen activation system in Alzheimer's disease: consequences on extracellular maturation of brain-derived neurotrophic factor and therapeutic implications. CNS Neurosci Ther 2019; 25: 303-313.
[38] Ng TKS, Ho CSH, Tam WWS, Kua EH and Ho RC. Decreased serum brain-derived neurotrophic factor (BDNF) levels in patients with Alzheimer's disease (AD): a systematic review and meta-analysis. Int J Mol Sci 2019; 20: 257.
[39] Hu E, Du H, Zhu X, Wang L, Shang S, Wu X, Lu H and Lu X. Beta-hydroxybutyrate promotes the expression of BDNF in hippocampal neurons under adequate glucose supply. Neuroscience 2018; 386: 315-325.
[40] Martinez BA, Petersen DA, Gaeta AL, Stanley SP, Caldwell GA and Caldwell KA. Dysregulation of the mitochondrial unfolded protein response induces non-apoptotic dopaminergic neurodegeneration in C. elegans models of Parkinson's disease. J Neurosci 2017; 37: 11085-11100.
[41] Kang MH, Das J, Gurunathan S, Park HW, Song H, Park C and Kim JH. The cytotoxic effects of dimethyl sulfoxide in mouse preimplantation embryos: a mechanistic study. Theranostics 2017; 7: 4735-4752.